Performance measurement of the 8-input SQUIDs for TES frequency domain multiplexing

doi: 10.1007/s10909-008-9771-0

Journal of Low Temperature Physics manuscript No.
(will be inserted by the editor)

S. Kimura[a] · **K. Masui**[a] · **Y. Takei**[a,b] · **K. Mitsuda**[a] · **N. Y. Yamasaki**[a] · **R. Fujimoto**[c] · **T. Morooka**[d] · **S. Nakayama**[e]

Performance measurement of the 8-input SQUIDs for TES frequency domain multiplexing

23.07.2007

Keywords TES microcalorimter, SQUID, Signal multiplex

Abstract We report on performance of 8-input superconducting quantum interference devices (SQUIDs) for multiplexing transition-edge sensor signals by using freqency-domain multiplexing. We found the typical critical current and the flux noise to be 17-19 μA and 0.7-1.1 $\mu\Phi_0/\sqrt{\mathrm{Hz}}$, respectively. We also measured the crosstalk current between the input coils of the SQUIDs, and found that the mutual inductance was consistent with the design value, 800 pH. We confirmed that the cross talk current due to the mutual inductance was reduced by the flux-locked-loop (FLL) feedback, and its reduction rate was consistent with $1/(1+\mathscr{L})$, where $\mathscr{L}$ is the FLL feedback gain. We also show the result of 2-channel DC-driven TES signals readout using the 8-input SQUIDs.

PACS numbers: 85.25.Dq,42.79.Sz,07.85.Fv

1 Introduction

An imaging array of transition-edge sensor (TES) X-ray microcalorimeters is the leading candidate of an imaging spectrometer for future X-ray astronomy missions, such as DIOS (Diffuse Intergalactic Oxygen Surveyer)[1], EDGE (Explorer of Diffuse emission and Gamma-ray burst Explosions)[2], Constellation-X[3], and

[a]Institute of Space and Astronautical Science (ISAS), Japan Aerospace Exploration Agency (JAXA), 3-1-1, Yoshinodai, Sagamihara, Kanagawa, 229-8510, Japan,
E-mail: kimura@astro.isas.jaxa.jp, Tel: +81-42-759-8152, Fax: +81-42-759-8455,
[b]Netherlands Institute for Space Reserch (SRON), Sorbonnelaan 2, 3584 CA Utrecht, the Netherlands,
[c]Graduate School of Natural Science & Technology, Kanazawa University, Kakuma, Kanazawa, Ishikawa, 920-1192, Japan,
[d]Seiko Instruments Agency Inc. (SII), 563 Takatsuka-Shinden, Matsudo, Chiba 270-2222, Japan,
[e]SII NanoTechnology Inc. (SIINT), 563 Takatsuka-Shinden, Matsudo, Chiba 270-2222, Japan

XEUS (X-ray Evolving Universe)[4]. Since TES microcalorimeters are operated at low temperature ($\sim$100mK), a readout method that multiplexes TES signals at the cold stage is required to reduce heat load through wirings for large format arrays (e.g. $>$ 1000 pixels).

Two different concepts of multiplex have been proposed; time-domain multiplex (TDM) and frequency-domain multiplex (FDM) . In TDM, TESs are read out sequentially by switching SQUIDs sequentially[5]. In FDM, TESs are biased with AC voltage and signal pulses are modulated by their bias frequencies. Currents from TESs are summed and coupled to a SQUID, then signals are demodulated by room temperature electronics. Three summing methods for FDM are proposed so far; current sum[6,7], a summing loop[8], and flux sum[9,10]. Recently, we designed and fabricated 8-input SQUIDs[11] for 8-chanel flux sum. In this paper, we present characterizations of the SQUIDs. We also show results of readout experiments of 2-channel DC-biased TESs as the first trial using the SQUIDs.

2 Characterizations of 8-input SQUIDs

2.1 Critical current and flux noise

Multi-input SQUID is a SQUID coupled with plural number of input coils. The TESs operated by AC bias of different frequencies and signals summed magnetically. We fabricated prototype of the 8-input SQUIDs (4 different designs[11]). A schematic diagram of the circuit to use the 8-input SQUID is shown in Fig. 1 (a). The output of an 8-input SQUID is connected to a 420-stage SQUID array amplifier, 420-SSA[12]. We show the relation between the magnetic field and the SQUID output voltage, i.e. so-called ϕ-V curve, of the 8-input SQUID in Fig. 1 (b), where the SQUID output voltage is measured by the input current of the 420 SSA. In Fig. 2, we show the relation between the bias current and the bias voltage (i.e. I-V curve) and the flux noise. The critical currents are 17 and 19 μA, and the flux noises are 0.7 and 1.1 $\mu\Phi_0/\sqrt{\mathrm{Hz}}$ at I_{sq} = 29 μA and 31 μA for two devices, respectively. The critical currents are within the designed range (10-20 μA), however, the noise is by a factor of two higher than the ideal-design value (0.5 $\mu\Phi_0/\sqrt{\mathrm{Hz}}$).

2.2 Crosstalk between input coils

Because multiple input coils are coupled to a SQUID washer, input coils are coupled to one another inductively through the SQUID and directly. Such mutual inductance M_{1-2} degrades the energy resolutions when two or more TESs are multiplexed[11]. The design values of $M_{1-2} = 800$ pH. However, it will effectively reduce to $M_{1-2}/(1+\mathscr{L})$, when a flux locked loop (FLL) feedback of a loop gain, $\mathscr{L}$, is turned on.

We imposed a sinusoidal current to one of the input coils, and measured the current in another input coil by amplifying it by a SSA amplifier. We used lock-in-amplifier technique to increase the signal to noise ratio. Fig. 3(a) and Fig. 4 show the diagram of the experimental setup and an example of results, respectively. We

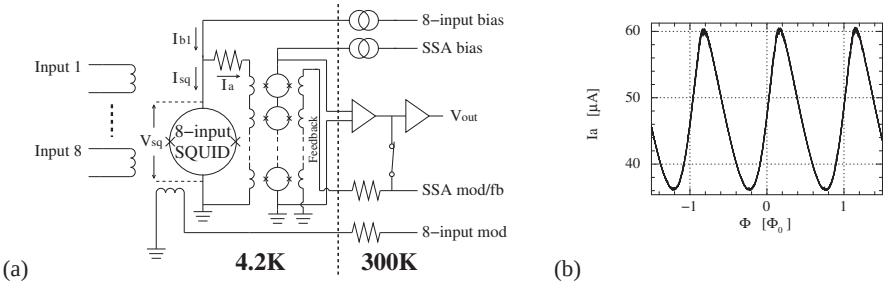

Fig. 1 (a) A schematic diagram of the circuit to read out signals using the 8-input SQUIDs. The output of the 8-input SQUID is amplified by a 420-stage SQUID. (b) Example of ϕ-V curve of the 8-input SQUID. The SQUID output voltage is shown by the input current to the 420 SSA.

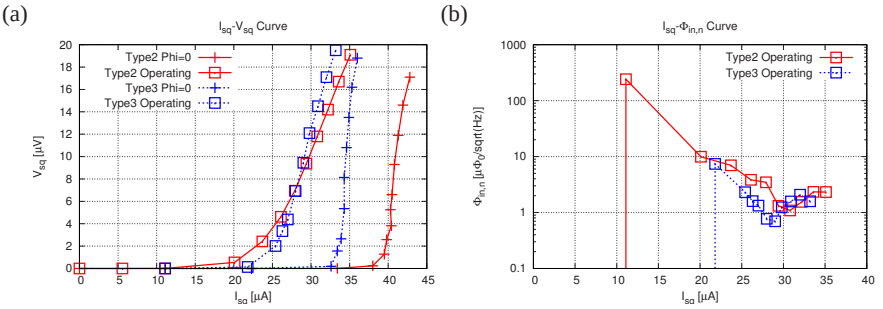

Fig. 2 (Color online) (a) I-V curves of two 8-input SQUIDs of different design[11] with 0 magnetic field (crosses) and with an offset magnetic field (boxes). Critical currents are 17 and 19 μA, respectively. (b) SQUID noise as a function of the bias current. The noise is 0.7 $\mu\Phi_0/\sqrt{\text{Hz}}$ for Type 3 ($I_{\text{sq}} = 29\ \mu$A) and 1.1 $\mu\Phi_0/\sqrt{\text{Hz}}$ for Type 2 ($I_{\text{sq}} = 31\ \mu$A).

find that the induced current decreases as the loop gain $\mathscr{L}$ increases for Fig. 4 (a), while its sign changes for (b). This overall behavior can be explained by a model which includes a stray inductance (Fig.3 (b)), and if the sign of the mutual inductance relative to the stray inductance is reversed to each other between Fig. 4 (a) and (b). In this model, the ratio of $I_{\text{in},2}$ to $I_{\text{in},1}$ follows

$$\frac{I_{\text{in},2}}{I_{\text{in},1}} = \frac{i\omega(\pm\frac{M_{1-2}}{1+\mathscr{L}} + M_{\text{st}})}{R_{\text{p}}} \tag{1}$$

and in the limit $\mathscr{L} \gg 1$, it saturates to

$$\frac{I_{\text{in},2}}{I_{\text{in},1}} = \frac{i\omega M_{\text{st}}}{R_{\text{p}}} \tag{2}$$

In this experiment, the AC current frequency was $f = 1$kHz, and we consider $R_{\text{p}} = 2-3$ mΩ from other measurements. From Eq. 2, we can estimate M_{st}. The ratio and phase shift expected from the model are shown in Fig. 4. We consider that model explains the overall behavior of the ratio and phase shift, though there are discrepancies at medium $\mathscr{L}$ data points.

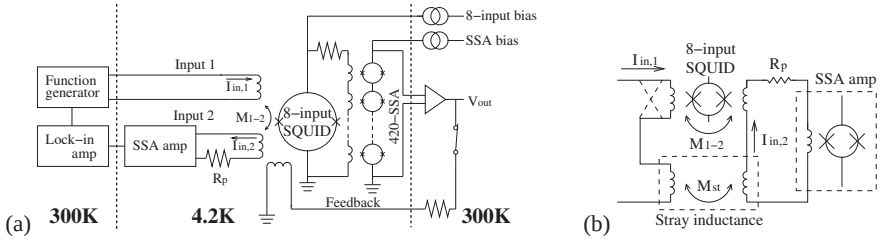

Fig. 3 (a) Schematic diagram of experimental setup to measure the crosstalk between two input coils. An AC current ($I_{\mathrm{in},1}$) applied to input coil 1 induces crosstalk current in other input coils ($I_{\mathrm{in},2}$), which is amplified by a 420 SSA. We used lock-in technology to increase signal to noise ratio. R_{p} is a residual resistance in the circuit connecting the input coils of the 8-input SQUID and the 420 SSA. We measured two cases, with the feedback of the 8-input on and off. (b) Stray inductance, M_{st}, are found to be necessary to explain the experimental results.

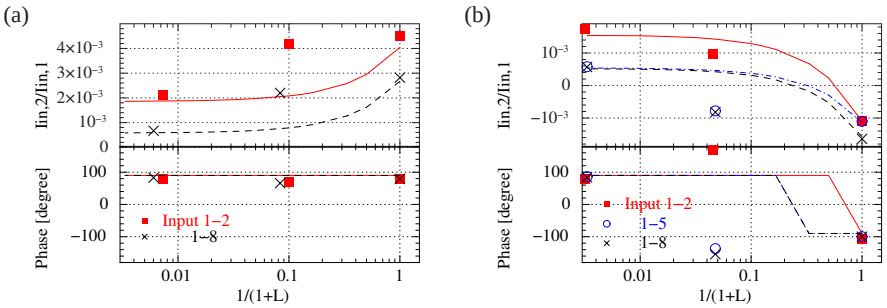

Fig. 4 (Color online) Ratio of the current induced in input coil 2 to the current imposed in input coil 1 (upper panel) and phase difference of the two (lower panel) as functions of the expected reduction factor by the FLL feedback. Data points (filled squares etc.) are measured values, while the solid and broken curves are the model based on the stray inductance assumption in Fig. 3 (b). Two panels, (a) and (b), are for two different SQUID.

3 Readout of 2-channel DC-driven TES signals

As an initial test of reading TES signals using the 8-input SQUID, we connected two TES microcalorimeters biased with DC voltages of opposite signs. The experimental set up using an adiabatic-demagnetization refrigerator (ADR) is shown in Fig. 5). While the operating temperature of the TESs is 80 mK, the the 8-input SQUIDs and the 420 SSA were mounted on the 1.3 K stage. We successfully detected signals from the two TES micorcalorimeters as shown in Fig. 6.

4 Conclusion

We demonstrated performance of the prototype devices of the 8-input SQUIDs. Both the critical current and the flux noise were close to the designed values. We also measured current induced in an input coil by the current imposed in another input coil. We found the induced current was suppressed by the FLL feedback

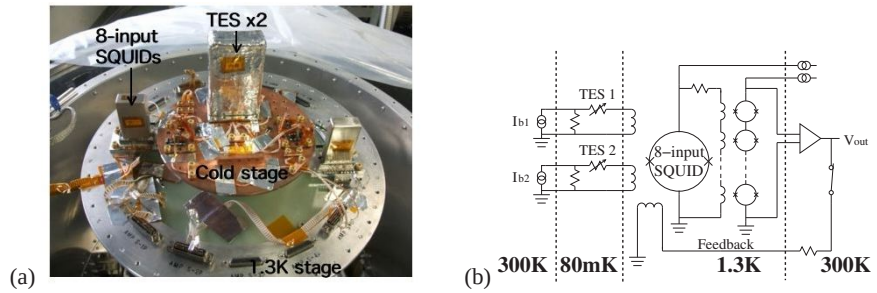

Fig. 5 (Color online) Experimental setup of reading 2 DC-biased TES. (a) Photograph of the cold stages. (b) Schematic diagram of the circuit.

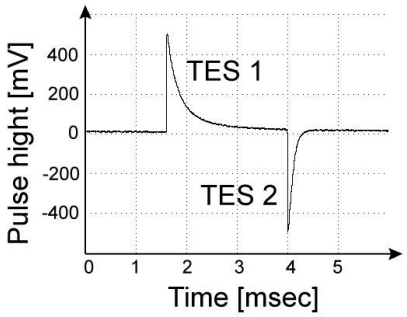

Fig. 6 Example of raw signal from the 8-input SQUID. Two TES happen to detect X-rays with a $\sim$ 2 ms interval. We can identify from the polarity of the signal which of the two TES have detected an X-ray.

and that the reduction rate was consistent with $1/(1+\mathscr{L})$. We also successfully obtained signals from two TES microcalorimeters.

References

1. T. Ohashi, et al., *Proc. SPIE*, **6266**, 18, (2006).
2. L. Piro, et al., a proposal submitted to ESA cosmic vision, (2007).
3. N. E. White, H. D. Tananbaum, A. E. Hornschemeier, M. R. Garcia, R. Petre, and J. A. Bookbinder, *Proc. SPIE*, **6266**, 62, (2006).
4. G. Hasinger, et al., *Proc. SPIE*, **6266**, (2006).
5. J. Chervenak, K. D. Irwin, E. N. Grossman, John M. Martinis, C. D. Reintsema, and M. E. Huber, *Appl. Phys. Lett.* **74**, 26, (1999).
6. J. van der Kuur, P.A.J. de Korte, H.F.C. Hoevers, M.P. Bruijn, M.L. Ridder, M. Kiviranta, and H. Seppa, *Nucl. Instrum. Methods. Res. A* **559**, 820, (2006).
7. T.M. Lanting, H.M. Cho, J. Clarke, W.L. Holzapfel, A.T. Lee, M. Lueker, P.L. Richards, M.A. Dobbs, H. Spieler, and A. Smith, *Appl. Phys. Lett.* **86**, 112511, (2005).
8. J. Yoon, J. Clarke, J.M. Gildemeister, A.T. Lee, M.L. Myers, P.L. Richards, and J.T. Skidmore, *Appl. Phys. Lett.* **78**, 3, (2001).

9. K. Mitsuda, R. Fujimoto, T. Miyazaki, K. Maegami, Y. Aruga, T. Oshima, S. Nakayama, S. Shoji, H. Kudo, Y. Yokoyama, T. Mihara, and H.M. Shimizu, *Nucl. Instrum. Methods. Res. A* **436**, 252, (1999).
10. K. Masui, Y. Takei, H. Ikeda, S. Kimura, K. Mitsuda, N.Y. Yamasaki, *Nucl. Instrum. Methods. Res. A* **559**, 811, (2006).
11. N.Y. Yamasaki, Y. Takei, K. Mitsuda, T. Morooka and S. Nakayama, *IEICE Trans. on Elec.* **E89-C**, 98, (2006).
12. T. Morooka, H. Myoren, S. Takeda, and K. Chinone, *Japanese J. Appl. Phys.* **42**, 6848, (2003).